Supplementary Information (SI) for Lab on a Chip.

Supplementary Information for

Programming hierarchical anisotropy in microactuators for multimodal actuation

Shiyu Wang, Shucong Li, Wenchang Zhao, Ying Zhou, Liqiu Wang*, Joanna Aizenberg*,

Pingan Zhu*

*Corresponding author. Email: liqiu.wang@polyu.edu.hk; jaiz@seas.harvard.edu;

pingazhu@cityu.edu.hk

Note S1: Morphologies of LCE microparticles

Uniform LCE microparticles could be fabricated using the microfluidics-enabled soft manufacturing method by controlling the inner-phase flow rate Q_i = 0.3-0.8 mL h^{-1} and outer-phase flow rate Q_o = 6-18 mL h^{-1}. The oil droplets encapsulated in the hydrogel microfibers are subjected to a compressive force along the radial direction. Thus, the resulting microparticles adopt a slender anisotropic shape with the long axis (LA) in the microfibers' axial direction and the short axis (SA) in the microfibers' radial direction.

As shown in **Figure S4**, the morphology of LCE microparticles can be engineered by tuning both Q_i and Q_o. The volume of LCE microparticles increases with the increase of Q_i and decreases with the increase of Q_o. The generated LCE microparticles are uniform in morphology, because of the capability of precisely manipulating small volumes of fluids by microfluidics.

A constant load can be applied to stretch the microfibers along the axial direction during the drying process. As such, the templated LCE microparticles will also be stretched to have a higher aspect ratio (defined as the length ratio between the LA and the SA). In this case, the cross-section of LCE microparticles can also be anisotropic in shape, for which two principal SAs are defined (e.g., SA1 and SA2). We used the length ratio of SA1 to SA2 (γ) to evaluate the cross-sectional anisotropy of the microparticles. Assuming that the length of SA1 is larger than that of SA2, we have $\gamma > 1$.

The influences of flow rates on the length of LA, SA1, and SA2 and the length ratio γ are shown in **Figure S6**. By keeping Q_o = 12 mL h^{-1} and increasing Q_i from 0.3 mL h^{-1} to 0.8 mL h^{-1}, the length of LA increases while that of SA2 remains nearly constant and the length of SA1 increases slightly. **Figure S7a** shows that the shape of LCE microparticles gradually changes from rod to strip, with the transition occurring between Q_i = 0.6 mL h^{-1} and Q_i = 0.7 mL h^{-1}. In contrast, Q_o has the opposite effect to Q_i on

changing the morphology of LCE microparticles, as shown in **Figure S6b**. By keeping Q_i = 0.6 mL h^{-1} and increasing Q_o from 6 mL h^{-1} to 18 mL h^{-1}, the length of LA decreases by ~320 μm (**Figure S6d**).

Supplementary Figures

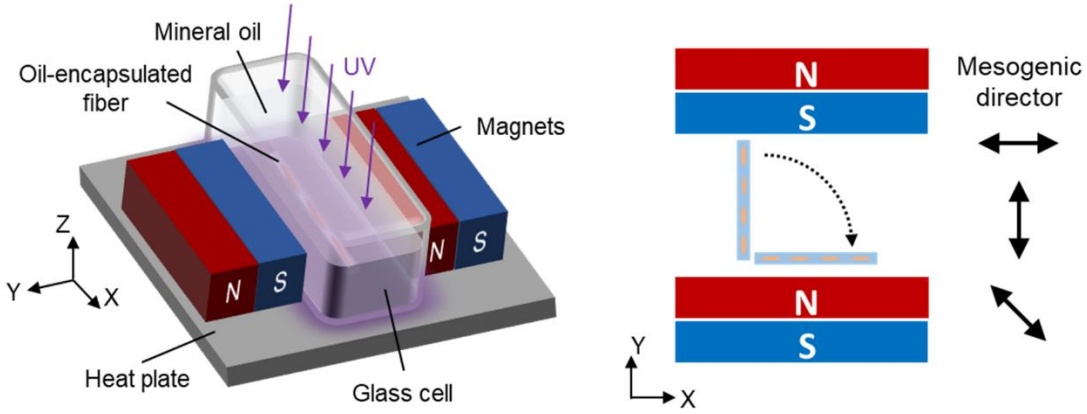

Figure S1. Schematic of the experimental setup for controlling the mesogenic director by a magnetic field during the polymerization.

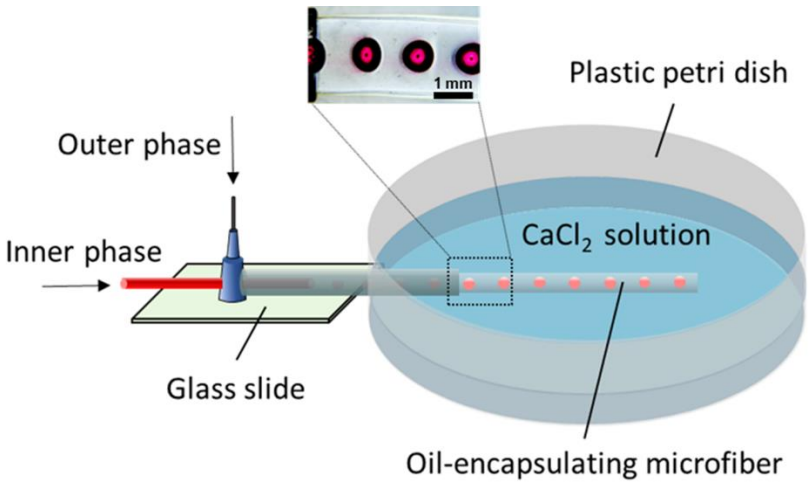

Figure S2. Schematic of the co-flow microfluidic device. Inset: micrograph showing the oil droplet array encapsulated in the hydrogel microfiber.

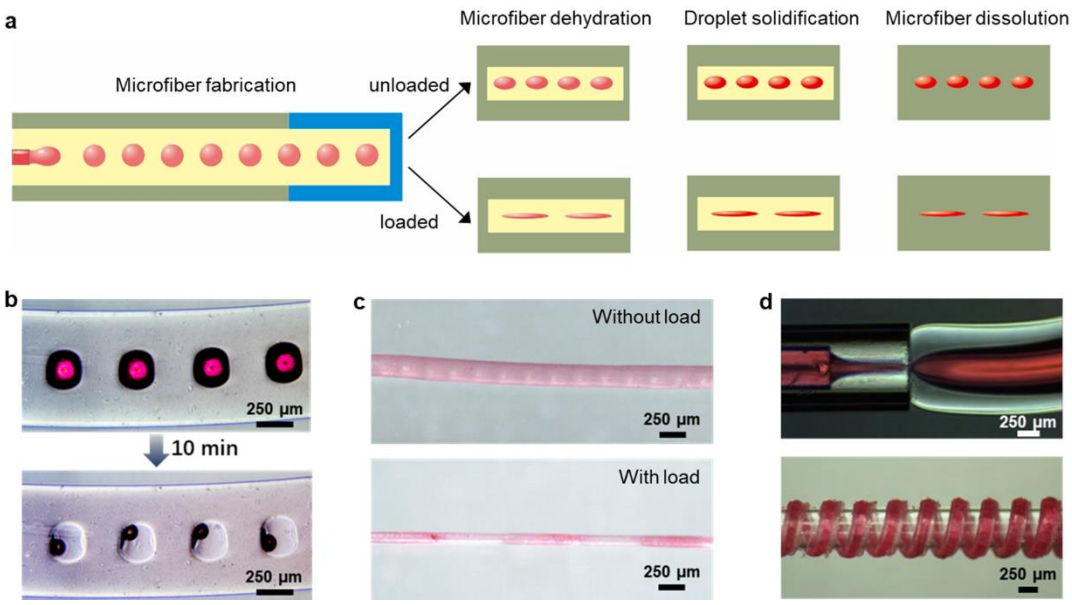

Figure S3. Microfiber-confined fabrication of LCE microstructures with anisotropic shapes. **a** Schematic of the four-step fabrication process: microfiber fabrication, microfiber dehydration, droplet solidification, and microfiber dissolution. **b** Optical images of the freshly prepared hydrogel microfiber (up) and the microfiber prepared after 10 mins (bottom). The evaporation of DCM leads to a reduction in the volume of the droplet and translates liquid droplets into solid particles. **c** Unloaded (up) and loaded (bottom) hydrogel microfibers after dehydration. **d** Optical images of an LCE jet encapsulated in a hydrogel microfiber (up) and an LCE microfiber wrapped around a glass capillary (bottom) for the preparation of helical LCE microfiber. The LCE is dyed red for better visualization in (**b**) to (**d**).

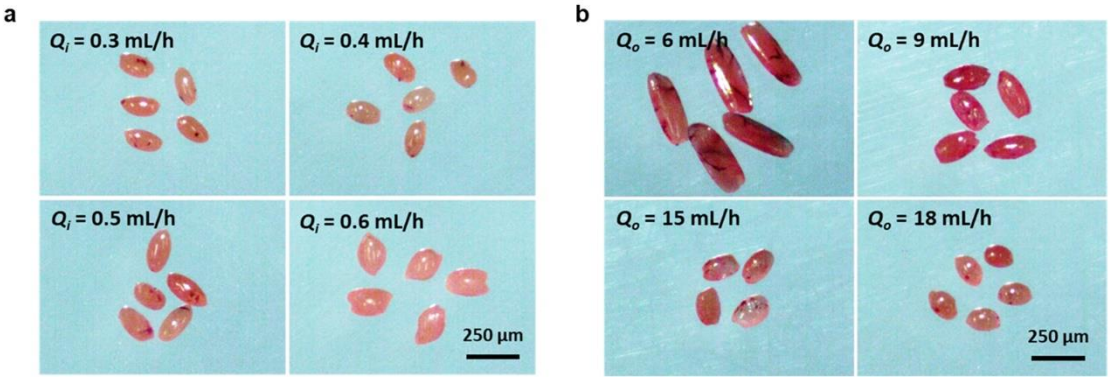

Figure S4. Morphologies of LCE microparticles templated from hydrogel microfibers. Optical images of LCE microparticles with varying flow rates of (**a**) the inner phase liquid Q_i (Q_o = 12 mL h^{-1}) and (**b**) the outer phase liquid Q_o (Q_i = 0.6 mL h^{-1}).

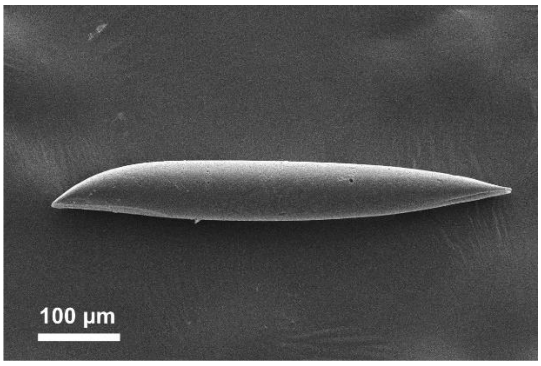

Figure S5. SEM image of the LCE micro-rod.

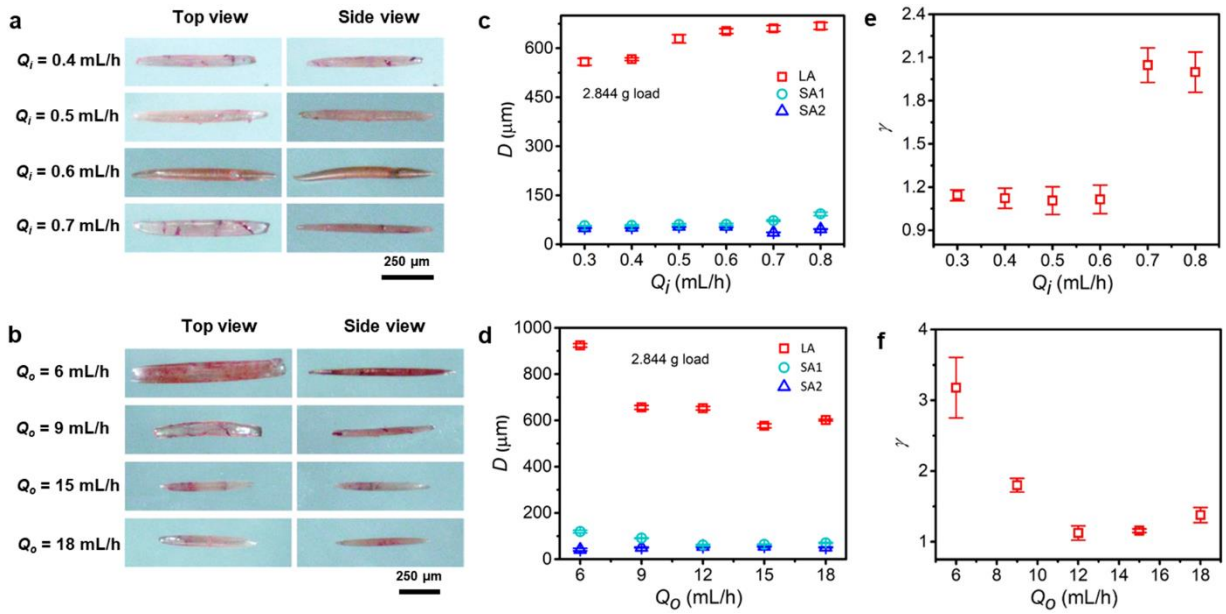

Figure S6. Controllable morphologies of LCE microparticles templated from hydrogel microfibers stretched by a load. The applied load is 2.844 g. **a** and **b** Optical images of LCE microparticles with varying flow rates of (**a**) the inner phase liquid Q_i (Q_o = 12 mL h^{-1}) and (**b**) the outer phase liquid Q_o (Q_i = 0.6 mL h^{-1}). **c** and **d** The length of the long axis (LA) and two principal short axes (PSA1 and PSA2), as controlled by varying (**c**) Q_i (Q_o = 12 mL h^{-1}) and (**d**) Q_o (Q_i = 0.6 mL h^{-1}). **e** and **f** The length ratio of the two principal axes γ controlled by varying (**e**) Q_i and (**f**) Q_o.

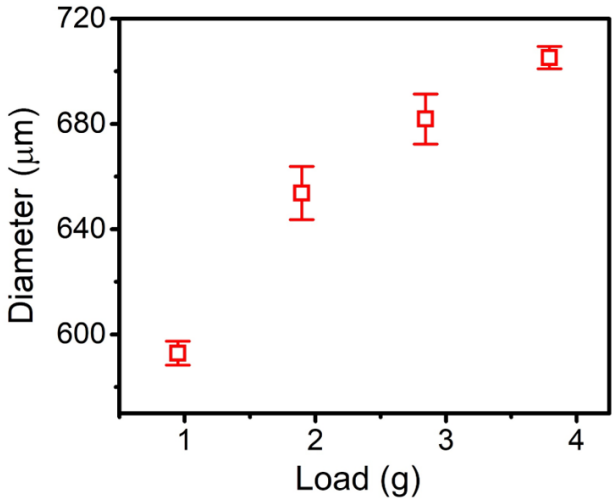

Figure S7. The length of LCE micro-rods versus the applied load. Q_o = 12 mL h^{-1} and Q_i = 0.6 mL h^{-1}.

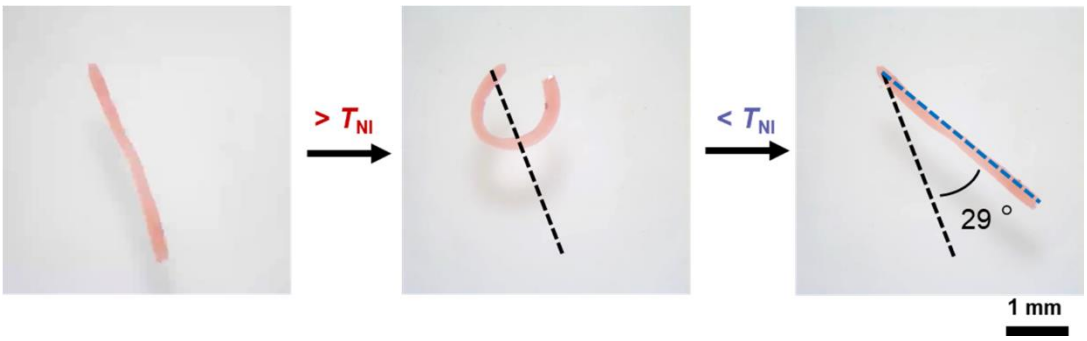

Figure S8. The rotational motion of an LCE micro-rod by large bending deformation undergoing a heating-cooling cycle. The black and blue dashed lines indicate the principal structural axis of the micro-rod before and after one cycle of bending actuation, respectively.

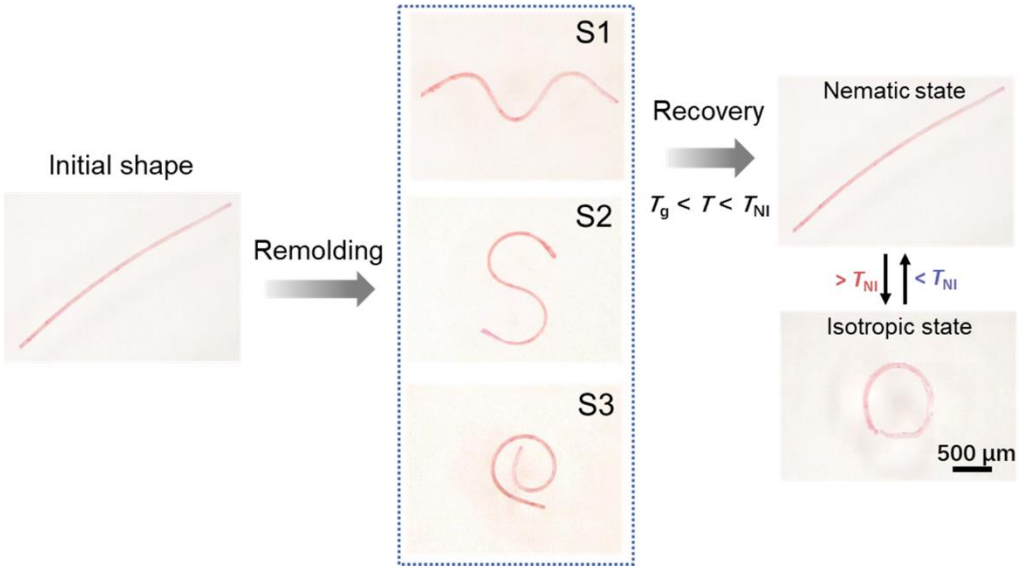

Figure S9. Programming temporary shapes of LCE microstructures by the shape memory effect. When the LCE is heated to a temperature T with $T_g < T < T_{NI}$, it can be temporarily remolded into arbitrary shapes (e.g., S1, S2, and S3) by external forces. The temporary shapes can be preserved by cooling until the structure is heated above T_g again.

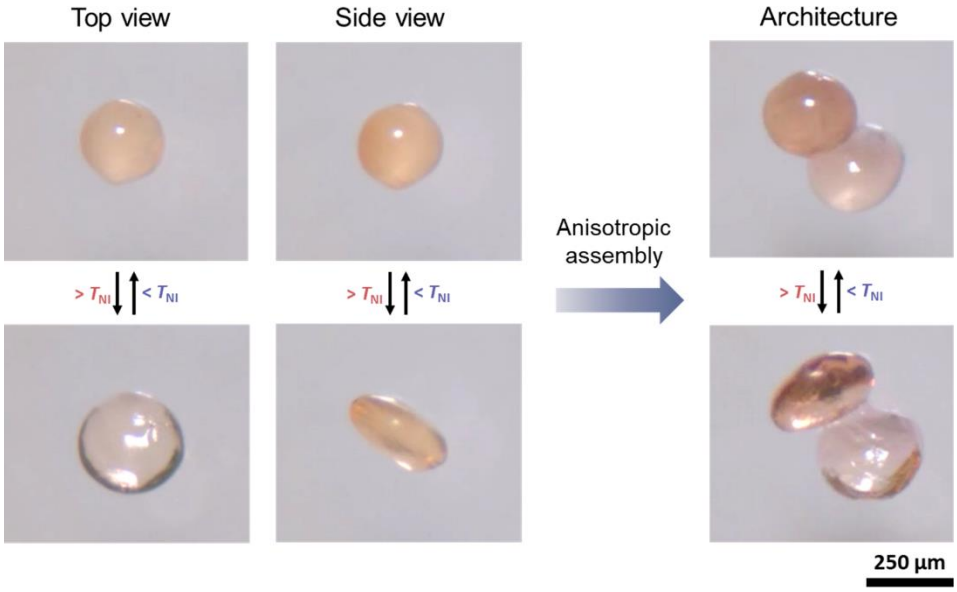

Figure S10. The anisotropic deformation by the assembly of isotropic LCE microspheres. Although LCE microspheres are isotropic in shape, the mesogenic alignment defines a well-controlled molecular anisotropy. The synergy between the molecular and architectural anisotropies leads to the anisotropic deformation of the assembled architecture. A variety of deformations can be further generated by varying the molecular or architectural anisotropy.

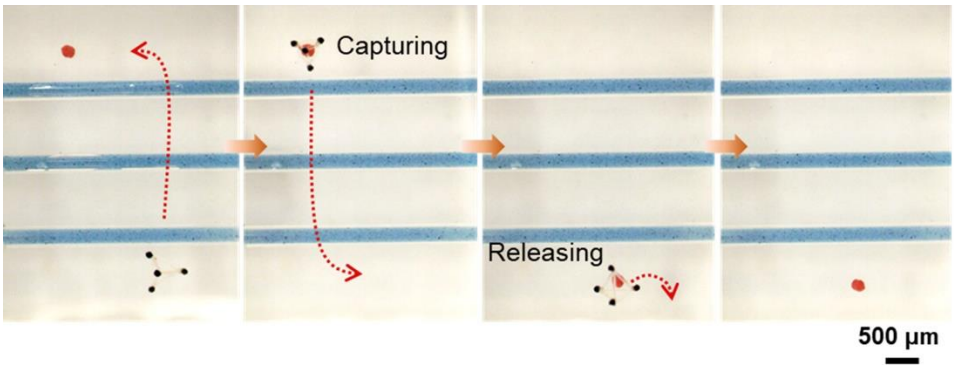

Figure S11. The tetrahedral microactuator capable of cargo transport over obstacles.